IEEE Access
Multidisciplinary | Rapid Review | Open Access Journal

Received April 24, 2018, accepted May 23, 2018, date of publication June 4, 2018, date of current version June 20, 2018.

Digital Object Identifier 10.1109/ACCESS.2018.2843780

Nano-Ferrite Near-Field Microwave Imaging for In-Body Applications

AIFENG REN[1], MAOJIE QING[1], NAN ZHAO[1], MINGMING WANG[1], GE GAO[1], XIAODONG YANG[1], ZHIYA ZHANG[1], FANGMING HU[1], MASOOD UR REHMAN[2], (Senior Member, IEEE), AND QAMMER H. ABBASI[3], (Senior Member, IEEE)

[1]School of Electronic Engineering, Xidian University, Xi'an 710071, China
[2]Department of Computer Science and Technology, University of Bedfordshire, Luton LU1 3JU, U.K.
[3]School of Engineering, University of Glasgow, Glasgow G12 8QQ, U.K.

Corresponding author: Xiaodong Yang (xdyang@xidian.edu.cn)

This work was supported in part by the International Scientific and Technological Cooperation and Exchange Projects in Shaanxi Province under Grant 2017KW-005, in part by the Fundamental Research Funds for the Central Universities under Grant JB180205, and in part by the National Natural Science Foundation of China under Grant 61671349, Grant 61301175, and Grant 61601338.

ABSTRACT In recent years, nanotechnology has become indispensable in our lives, especially in the medical field. The key to nanotechnology is the perfect combination of molecular imaging and nanoscale probes. In this paper, we used iron oxide nanoparticles as a nanoprobe because it is widely used in clinical MRI and other molecular imaging techniques. We built our own experimental environment and used absorbing materials during the whole experiment to avoid electromagnetic interference with the surroundings. Moreover, we repeated the experiment many times to exclude the influence of contingency. Hence, the experimental data we obtained were relatively precise and persuasive. Finally, the results demonstrated that the iron oxide nanoparticles were appropriate for use as contrast agents in biological imaging.

INDEX TERMS Nanotechnology, molecular imaging, nano probe, iron oxide nanoparticles.

I. INTRODUCTION

In today's society, medical technology has been extensively developed, but doctors still lack treatments for some critical diseases, especially cancer. Thus, better understanding of early diagnoses and accurate therapy for critical diseases, especially tumors, is key to improving the quality of life for patients. Traditional diagnostic imaging techniques and treatments have been unable to meet increasingly sophisticated requirements, and molecular imaging emerged at a historic moment. The concept of molecular imaging was first proposed by Weissleder in 2001. Molecular imaging is one of the latest cross-disciplinary branches spanning contemporary physics, chemistry, molecular biology, information technology, clinical medicine and medical imaging techniques, and it can achieve non-invasive and in vivo real-time dynamic imaging of the processes of internal physiological or pathological processes in cells, at the genetic and molecular levels. The primary applications of molecular imaging are photoacoustic imaging (PA), magnetic resonance imaging (MRI), magnetomotive ultrasound imaging (MMUS), positron emission tomography (PET), computed tomography (CT), and single-photon-emission computed tomography (SPECT).

Molecular imaging has been applied to various fields. Yaohong Zhao's research group used molecular probes to investigate the surface structure of metal passivator on copper [1]. Metal passivator molecular probes were obtained by introducing specific substituents to a benzotriazole skeleton. Then, they evaluated the inhibition effectiveness of the molecular probe through a corrosive aging test with dibenzyl disulfide. Surface analyses of copper treated with the molecular probe were conducted via scanning electron microscopy/energy dispersive X-ray spectroscopy (SEM/EDX), Fourier transform infrared spectroscopy (FTIR) and X-ray photoelectron spectroscopy (XPS). Janusz H. Hankiewicz's research group used zinc-doped copper ferrite particles as temperature sensors for magnetic resonance imaging (MRI) [2]. They found that $Cu_{0.35}Zn_{0.65}Fe_2O_4$ has a Curie temperature near body temperature (290 K), and it produced significant changes in the MRI intensity as a function of temperature. The temperature resolution was approximately 1.3 K. Hsin-Chih Yeh's research group invented a new molecular probe for the homogenous detection of nucleic acid targets [3]. They discovered that interactions between

oligonucleotide-templated nanoclusters consisting of a few atoms of silver (DNA/Ag NCs) and a proximal, guanine-rich DNA strand led to tremendous red fluorescence enhancement. They found that dark silver nanoclusters templated on ssDNA could be illuminated to exhibit a palette of colors (green, yellow, red) by employing different proximal sequences.

Molecular imaging is most commonly used to diagnose and validate critical diseases. The formulation and accumulation of extracellular amyloid-beta peptide aggregates in the brain are associated with Alzheimer's disease. Apostolos C. Tsolakis's research group synthesized and characterized a multi-functional non-toxic and biodegradable nanomaterial (iron oxide nanoparticles, Fe_3O_4, ~10 nm, coated with silica SiO_2 and Thioflavin-T) [4], which can be used to bind amyloid-beta peptides, providing a way to visualize and potentially inhibit their aggregation. Therefore, nanoparticles offer a way to accurately diagnose and effectively treat Alzheimer's disease.

The sentinel lymph nodes (SLNs) are the first regional lymph node that drains into the primary tumor, and if cancer has spread, it is likely to find metastases in the SLNs. Maria Evertsson's research group used superparamagnetic iron oxide nanoparticles (SPIO-NPs) as a contrast agent [5], and then they utilized both the frequency and phase-gated magnetomotive ultrasound (MMUS) algorithm and conventional magnetic resonance imaging (MRI) to monitor rat SLNs. The results demonstrated that their method could be used for bedside guidance during SLN surgery. Michael Bietenbeck's study demonstrated that MRI enabled an accurate assessment of both functional and structural cardiac parameters, leading to the appropriate diagnosis and validation of cardiovascular diseases [6]. Iron oxide nanoparticles open up new research opportunities such as remote magnetic drug targeting (MDT). Min Lu's research group determined that iron oxide nanoparticles could be used as magnetic particle imaging tracers for therapy in adult patients with chronic kidney disease [7].

II. NANO PROBE

The core of molecular imaging is perfect fusion of an appropriate nano probe and an imaging device with fast speed, high sensitivity, and high resolution. The ideal molecular imaging probe meets the following conditions [8]: (1) highly specific binding capacity and good affinity for the target; (2) good permeability so it can quickly pass through the biological barrier; (3) does not lead to obvious immune response by the organism; and (4) able to couple with signaling molecules. The nano-molecular probe system consists of three parts [9], namely, the nanoparticle carrier, molecular markers and modified molecule, and the topology is shown in Fig. 1. Nano probes used as contrast agents have improved images of the heart, focal liver lesions, kidney, and breast tumor vasculature, among numerous other applications [10]. An illustration of a nano probe attached to a tumor or DNA is shown in Fig. 2.

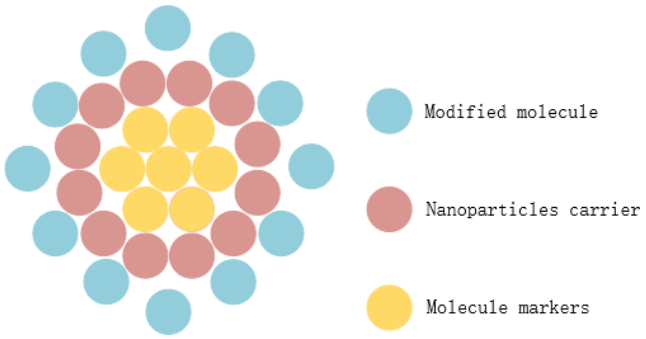

FIGURE 1. Nano-molecular probe system.

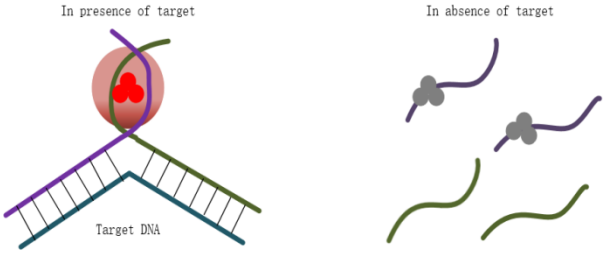

FIGURE 2. Example of the fluorescent nanoscale probe. The nanoscale probe fluoresces in the presence of target DNA.

In this paper, we used oxide nanoparticles as a nano probe. From Antje Lindemann's research, we knew that dextran-coated superparamagnetic iron oxide nanoparticles (SPIONs) had good labeling efficiencies and cytosolic accumulation [11]. In previous studies, magnetic particle imaging (MPI) was demonstrated to be a promising medical imaging technology that used iron oxide nanoparticles as clinically safe tracers [12], [13].

Nahrendorf's research group fabricated a target probe [14], and they coupled a new type of polypeptide to SPIONs. These polypeptides could be combined with specific adhesion molecules on endothelial cells and macrophages from an atherosclerotic lesion site. Using such a probe enables the early detection of lesions in patients who have had carotid plaques excised by MRI. Vernimmen's research group fabricated a folate-SPION probe by adding folate to the surface of SPIONs [15]. This type of nano probe can significantly increase tumor uptake of folate-SPIONS, improving the detection rate of tumors by MRI. Yong-Min Huh's research group fabricated a Herceptin-SPION probe that can target human epidermal growth factor receptor [16]. For mice injected with Herceptin-SPION probes, due to the accumulation of probes at the tumor site, the relaxation signal at the tumor site had a remarkable change. However, mice injected with pure SPION probes under the same conditions showed no obvious change in the signal at the tumor site.

In this experiment, we used strontium ferrite as a contrast agent. The chemical formula of strontium magneto plumbite ferrite is $SrFe_{12}O_{19}$, and a single cell of strontium magneto plumbite ferrite contains two molecules. Sr^{2+} is a divalent metal cation, Fe^{3+} is a trivalent metal cation, and oxygen ions are packed in six corners. In general, the critical point of

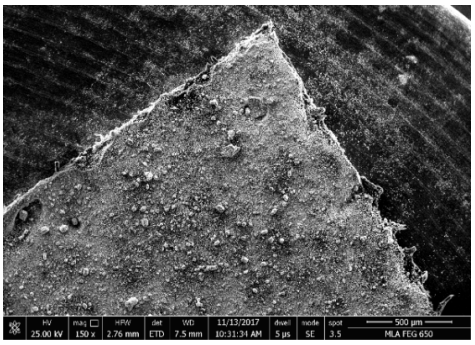

(a)

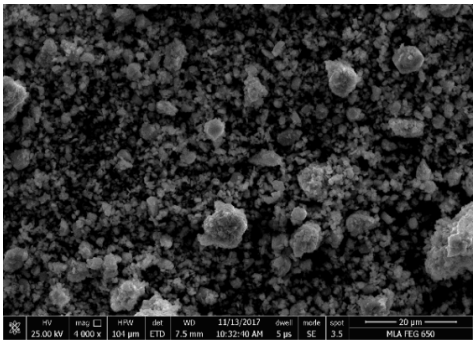

(b)

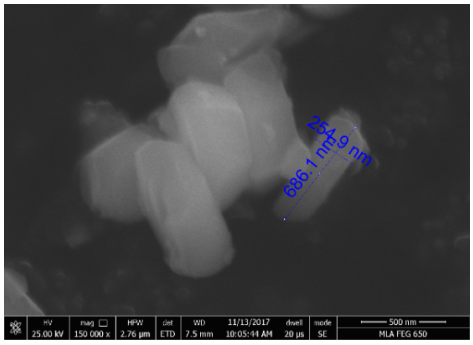

(c)

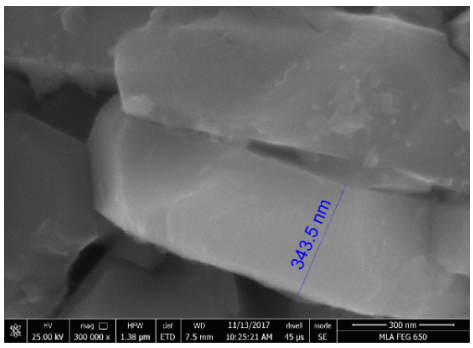

(d)

FIGURE 3. Electron micrographs of strontium ferrite. Overview of strontium ferrite, where the magnification of (a) is 150 times and the magnification of (b) is 4000 times. (c) and (d) are details of strontium ferrite with the size of the particles marked: magnification of (c) is 150,000 times and magnification of (d) is 300,000 times.

superparamagnetism of ferrite particles is about 30 $\sim$ 70nm, but if it is a porous cluster, it can also show superparamagnetism at a few hundred nanometers. The electron micrographs of strontium ferrite are shown in Fig. 3. Strontium magneto plumbite ferrite with its hexagonal structure has many excellent properties [17], including a high performance to price ratio, high Curie temperature, high coercive force, high saturation magnetization, high magnetic energy product, uniaxial magnetocrystalline anisotropy, and good mechanical hardness and chemical stability. It has been widely used for the preparation of high-density perpendicular magnetic recording materials, permanent magnetic materials, magneto-optical devices, microwave devices, and electromagnetic shielding materials, which play important roles in scientific research and industrial production.

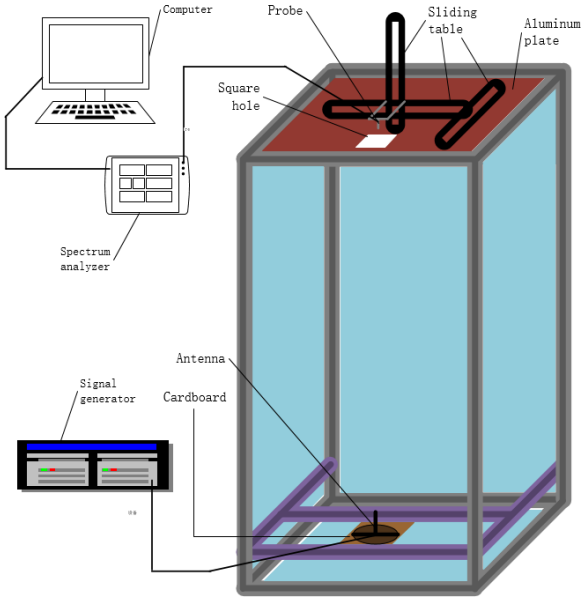

FIGURE 4. Schematic of the experimental setup.

III. EXPERIMENTAL SETUP AND PROCEDURES

The entire experimental structure is shown in Fig. 4. The cube in Fig. 4 is a framework made of aluminum profiles. From the figure, the eight gray horizontal aluminum rods at the top and the bottom are 60 cm long, and the four gray vertical aluminum rods used to connect the top and bottom are 120 cm long. Furthermore, we can clearly see that there are four purple horizontal aluminum rods, with a length of 60 cm, which is the same as that of the aluminum rods at the top and bottom. Their position in the whole structure is adjustable, and they are used to adjust the distance between the antenna and the sample. The brown parallelogram between two purple horizontal aluminum rods represents a piece of cardboard used to place an antenna. The black ellipse on the cardboard represents the base of the antenna, and the vertical symbol in close proximity to the black ellipse represents the antenna. The base of the antenna is connected to the signal generator. We used the signal generator to produce stable electromagnetic waves.

From Fig. 4, the red surface at the top of the cube represents an aluminum plate. The five other surfaces, represented as

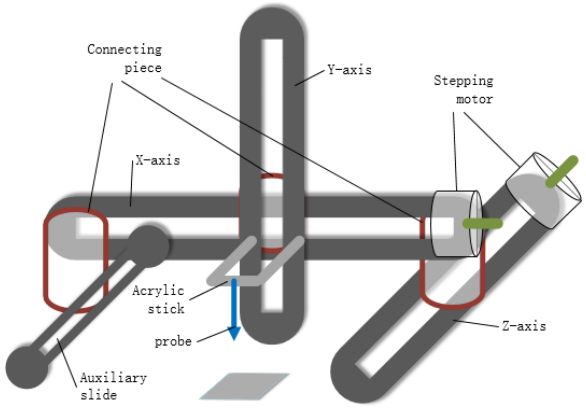

FIGURE 5. Detailed diagram of sliding tables and probe.

blue areas, indicate the placement of materials that absorbed electromagnetic waves on these five surfaces.

The absorbing materials were used to create an anechoic chamber to isolate samples from the electromagnetic interference of the surroundings. We made a square hole, 5 mm from each edge of the aluminum plate, and the position of the square hole is shown in Fig. 4. It was used to place the sample, and then we used a probe to scan the sample. The probe is placed above the square hole, as shown in Fig. 4. The probe is fixed on sliding tables, and the sliding tables are fixed to the aluminum plate using screws. During the experiment, we manipulate the sliding tables to control the movement of the probe, moving the probe to scan the sample. A detailed diagram of the sliding tables and probe is shown in Fig. 5. The probe is connected to a spectrum analyzer, and the spectrum analyzer is connected to the computer via an Ethernet cable.

A detailed diagram of the sliding tables is shown in Fig. 5, and it is similar to a previously reported setup [17], [18]. There are three tables that could slide in the X, Y and Z directions and an auxiliary slide, which is parallel to the sliding table of the Z-axis. The tables that slide along the X-axis and Z-axis are 300 mm long, while that of the Y-axis is 200 mm. The two cylindrical objects in Fig. 5 represent two stepping motors. The X-axis sliding table and the Z-axis sliding table are both connected to a stepping motor at one end, while the Y-axis sliding table is not connected to the stepping motor.

There are two acrylic sticks parallel to the Z-axis sliding table, and they are fixed on the Y-axis sliding table. These two acrylic sticks enable us to fasten one acrylic stick parallel to the X-axis sliding table. Afterwards, we fix the probe on the acrylic stick parallel to the X-axis sliding table, and the blue arrow in Fig. 5 represents the probe. Furthermore, the three dark red rounded rectangles in the figure represent connecting pieces between the sliding tables or between the sliding table and auxiliary slide.

During the experiment, the power of the electromagnetic wave was 5 dBm and the frequency of the electromagnetic wave was 3.5 GHz; therefore, the wavelength is approximately 9 cm. From Fig. 4, the adjustable four purple aluminum rods maintain a distance between the antenna and sample that is 10 times greater than the wavelength of the electromagnetic wave. Those four purple aluminum rods are placed as close as possible to the bottom. Because the absorbing material needs to be placed at the bottom, we reserved some space. Finally, we adjusted the distance between the bottom and four purple aluminum rods to 10 cm, so the distance between the top and those four purple aluminum rods is 110 cm. Given the height of the antenna, the distance between the antenna and the sample is approximately 105 cm, which is greater than 10 times the wavelength of the electromagnetic wave (90 cm).

For clear results, we used agar instead of organisms, because agar is relatively uniform. Before the experiment, we cultivated the agar in a culture dish. We mixed 150 ml water with 1 g agar, and the temperature of the water was greater than 90°C. First, we fully stirred the mixture of water and agar in a beaker to guarantee no precipitation; second, we poured the mixture into a clean culture dish; and finally, we covered the lid and allowed the mixture to completely cool and condense into a semisolid state. The diameter of the culture dish was 7 cm. Before the experiment was conducted, we aligned the center of the culture dish with the center of the square hole, and then we calibrated the position of the probe so that it was appropriately located.

At the beginning of the experiment, the probe was located in the upper left of the culture dish. First, the stepping motor connected to the X-axis sliding table rotated clockwise, which drove the Y-axis sliding table to move along the X-axis, moving the probe along the X-axis. When moving to the appropriate position, the stepping motor stopped rotating, generating a line of data. Then, the stepping motor connected to the Z-axis sliding table and rotated a small step counterclockwise, which drove the X-axis sliding table to move along the Z-axis, making the probe a small step along the Z-axis. Finally, the stepping motor connected to the Z-axis sliding table and stopped rotating, while the stepping motor connected to the X-axis sliding table rotated counterclockwise, which drove the Y-axis sliding table to move against the X-axis, making the probe move against the X-axis. The stepping motor connected to the X-axis sliding table stopped rotating until the coordinate of the probe on the X-axis was the same as that at the beginning of the experiment. We then repeated this process 39 times, to generate 40 lines of data, with 380 columns of data per line. During the whole experiment, the coordinate of the probe on the Y-axis was invariable, that is, the distance between the probe and agar remained constant. Every time we collected data, the probe was reset to carry out the next experiment.

IV. RESULTS AND DISCUSSION

As shown above, the frequency of the electromagnetic wave we used was 3.5 GHz. The electromagnetic interference near 3.5 GHz from the surroundings was relatively small, and we used absorbing materials to create an anechoic chamber to eliminate electromagnetic interference from

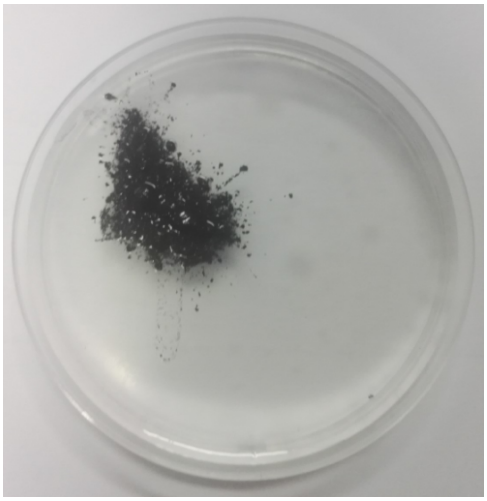

FIGURE 6. Ferrite was placed on the upper left corner of the agar.

the surroundings. Furthermore, the distance between the antenna and the sample was approximately 105 cm, which was 10 times greater than the wavelength of the electromagnetic wave; therefore, the electromagnetic wave could be approximated as a plane wave when it arrived at the sample. Combining the above two points, the results were relatively stable and accurate.

First, we used the probe to scan the agar without ferrite. The principle and process of the experiment are described earlier. After 40 lines of data were collected, we reset the probe. Then, we used the collected data to draw a grayscale map, as shown in Fig. 7(a). Later, we laid the ferrite on the upper left corner of the agar as evenly as possible, as shown in Fig. 6. We also ensured that the relative positions of the culture dish and the square hole were the same as when no ferrite was present. Then, we collected data in the same way. We reset the probe when we finished collecting 40 lines of data, and then we used the collected data to draw another grayscale map, as shown in Fig. 7(b).

In these two grayscale maps (Fig. 7), light colors indicate more energetic electromagnetic waves measured by the probe, while darker colors indicate less energetic electromagnetic waves measured by the probe. Without ferrite, (Fig. 7[a]) there was a black band in the upper left corner, that is, an area that received less energy than other areas. We first considered the non-uniformity of the agar to have caused this phenomenon. Then, after recultivating the agar and repeating the experiment many times, we found that the results were all similar, confirming that this phenomenon was not caused by non-uniformity of the agar. Next, we considered whether this lower energy area was caused by the antenna. We changed the position of the antenna and repeated the experiment, determining that the results differed. Therefore, the uneven electromagnetic waves emitted by the antenna caused this result. Fig. 7(b) shows the agar with ferrite, which was placed on the upper left corner of the agar. The black band in the upper left corner was not as obvious as in Fig. 7(a), and it

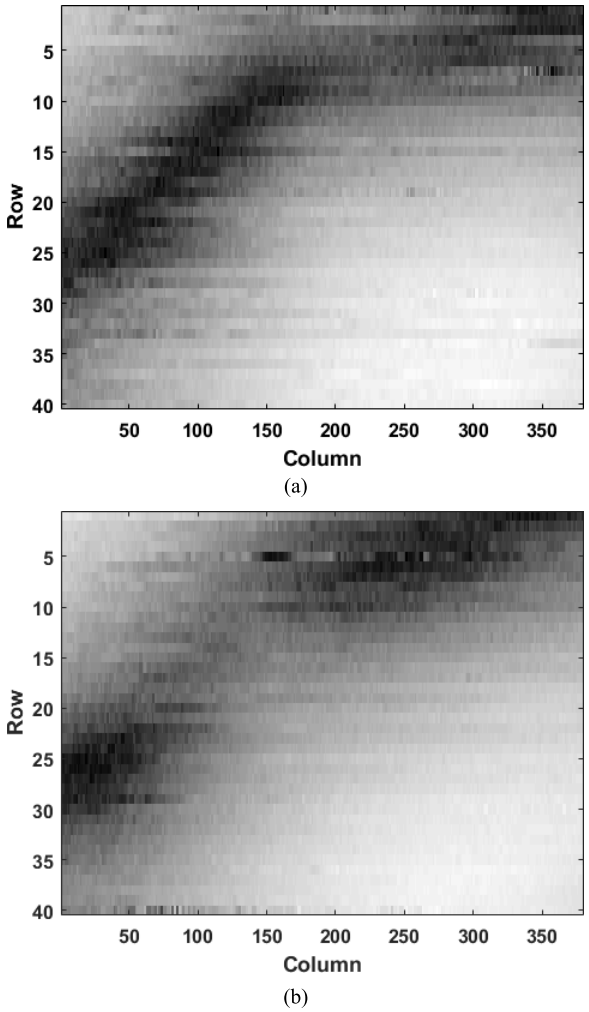

FIGURE 7. Images were acquired under a frequency of 3.5 GHz and power of 5 dBm. (a) No ferrite on the agar, and (b) ferrite on the upper left corner of the agar.

appeared that the band was cut off from the middle. Furthermore, the missing part of the black band was exactly where the ferrite was located, confirming that the ferrite caused the differences observed between Fig. 7(a) and Fig. 7(b).

Later, we subtracted the experimental data from the agar with ferrite from that of the agar without the ferrite, and then we drew the grayscale map shown in Fig. 8. The red marked area in Fig. 8 is clearly lighter than the rest of the figure, and that area corresponded to the location of the ferrite. This triangle also matched the shape of the ferrite on the agar. However, the actual shape of the ferrite was not exactly the same as that on the grayscale map because the triangle was deformed by refracted and reflected electromagnetic waves.

Now it's just the preliminary stage, the frequency of the electromagnetic is low so the resolution is relatively low. From Figure 4 we can see that the top of the experimental device is a piece of aluminum plate, it is known that the metal has a strong refraction and reflection on electromagnetic wave. In the future, we will remove the aluminum plate, in this case, the refraction and reflection effects of

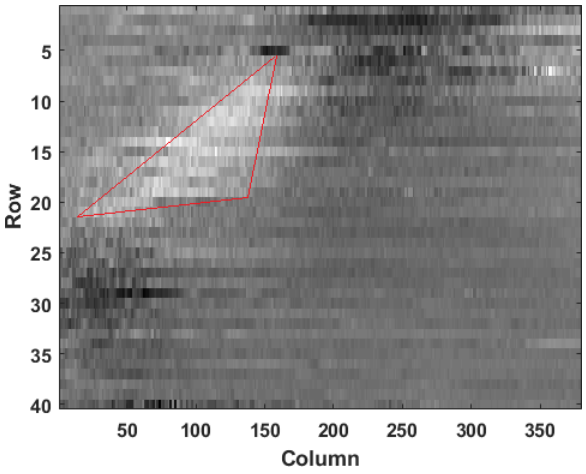

FIGURE 8. Image generated by subtracting the two sets of data.

electromagnetic waves can be greatly reduced, and the grayscale images will be more close to the actual shapes.

In this study, we have shown that iron oxide nanoparticles absorb electromagnetic waves well. There was also good biological affinity that will not lead to an immune response by the organism. Therefore, iron oxide nanoparticles are good nano probes to be utilized in magnetic resonance imaging (MRI) and magnetic drug targeting (MDT).

V. CONCLUSION

In summary, we used agar to replace organisms and then utilized strontium ferrite as a contrast agent to conduct this experiment under an emission frequency of 3.5 GHz with emission power of 5 dBm. We used the experimental data to draw the grayscale maps. Based on the experimental results and previous studies, we determined that iron oxide is very suitable as a nano probe for the early diagnosis and accurate treatment of various diseases, especially cancer. Nanotechnology will certainly play an increasingly more important role in the future of biological imaging and the medical field.

REFERENCES

[1] Y. Zhao, Y. Qian, W. Su, and X. Chen, "Application of molecular probe to investigate surface structure of metal passivator on copper," *IEEE Trans. Dielectr. Electr. Insul.*, vol. 23, no. 2, pp. 1142–1147, Apr. 2016.

[2] J. H. Hankiewicz *et al.*, "Zinc doped copper ferrite particles as temperature sensors for magnetic resonance imaging," *AIP Adv.*, vol. 7, no. 5, p. 056703, May 2017.

[3] H.-C. Yeh, J. Sharma, J. J. Han, J. S. Martinez, and J. H. Werner, "NanoCluster Beacon—A new molecular probe for homogeneous detection of nucleic acid targets," in *Proc. IEEE Int. Conf. Nano/Micro Eng. Mol. Syst.*, Kaohsiung, Taiwan, Feb. 2011, pp. 267–270.

[4] A. C. Tsolakis *et al.*, "Magnetic fluorescent nanoparticles binding to amyloid-beta peptide: Silica-coated, Thioflavin-T functionalized iron oxide," *IEEE Trans. Magn.*, vol. 53, no. 11, Nov. 2017, Art. no. 5300804.

[5] M. Evertsson *et al.*, "Multimodal detection of iron oxide nanoparticles in rat lymph nodes using magnetomotive ultrasound imaging and magnetic resonance imaging," *IEEE Trans. Ultrason., Ferroelectr., Freq. Control*, vol. 61, no. 8, pp. 1276–1283, Aug. 2014.

[6] B. Michael *et al.*, "Remote magnetic targeting of iron oxide nanoparticles for cardiovascular diagnosis and therapeutic drug delivery: Where are we now?" *Int. J. Nanomed.*, vol. 11, pp. 3191–3203, Jul. 2016.

[7] M. Lu, M. H. Cohen, D. Rieves, and R. Pazdur, "FDA report: Ferumoxytol for intravenous iron therapy in adult patients with chronic kidney disease," *Amer. J. Hematol.*, vol. 85, no. 5, pp. 315–319, Jan. 2010.

[8] R. Weissleder and U. Mahmood, "Molecular imaging," *Radiology*, vol. 219, no. 2, pp. 316–333, May 2001.

[9] B.-G. Ye and Y. Ling, "Principle and realization of Nano-molecular probe in molecular imaging technologies," in *Proc. Int. Conf. Bioinf. Biomed. Eng.*, Beijing, China, 2009, pp. 2335–2338.

[10] D. Hyun *et al.*, "Improved sensitivity in ultrasound molecular imaging with coherence-based beamforming," *IEEE Trans. Med. Imag.*, vol. 37, no. 1, pp. 241–250, Jan. 2018.

[11] A. Lindemann, R. Pries, K. Lüdtke-Buzug, and B. Wollenberg, "Biological properties of superparamagnetic iron oxide nanoparticles," *IEEE Trans. Magn.*, vol. 51, no. 2, Feb. 2015, Art. no. 5200204.

[12] H. Arami and K. M. Krishnan, "Highly stable amine functionalized iron oxide nanoparticles designed for magnetic particle imaging (MPI)," *IEEE Trans. Magn.*, vol. 49, no. 7, pp. 3500–3503, Jul. 2013.

[13] R. M. Ferguson *et al.*, "Magnetic particle imaging with tailored iron oxide nanoparticle tracers," *IEEE Trans. Med. Imag.*, vol. 34, no. 5, pp. 1077–1084, May 2015.

[14] M. Nahrendorf *et al.*, "Noninvasive vascular cell adhesion molecule-1 imaging identifies inflammatory activation of cells in atherosclerosis," *Circulation*, vol. 114, no. 14, pp. 1504–1511, Oct. 2006.

[15] D. Vernimmen, M. Gueders, S. Pisvin, P. Delvenne, and R. Winkler, "Different mechanisms are implicated in ERBB2 gene overexpression in breast and in other cancers," *Brit. J. Cancer.*, vol. 89, no. 5, pp. 899–906, Sep. 2003.

[16] Y.-M. Huh *et al.* "*In vivo* magnetic resonance detection of cancer by using multifunctional magnetic nanocrystals," *J. Amer. Chem. Soc.*, vol. 127, no. 35, pp. 12387–12391, Sep. 2005.

[17] K. W. Jeon *et al.*, "Synthesis and magnetic properties of aligned strontium ferrites," *IEEE Trans. Magn.*, vol. 50, no. 6, pp. 1–4, Jun. 2014.

[18] M. Tabib-Azar, J. L. Katz, and S. R. LeClair, "Evanescent microwaves: A novel super-resolution noncontact nondestructive imaging technique for biological applications," *IEEE Trans. Instrum. Meas.*, vol. 48, no. 6, pp. 1111–1116, Dec. 1999.

[19] K. Hoshino, A. Gopal, and X. Zhang, "Near-field scanning nanophotonic microscopy—Breaking the diffraction limit using integrated nano light-emitting probe tip," *IEEE J. Sel. Topics Quantum Electron.*, vol. 15, no. 5, pp. 1393–1399, Sep./Oct. 2009.

AIFENG REN is currently with the School of Electronic Engineering, Xidian University.

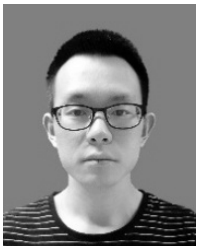

MAOJIE QING is currently pursuing the master's degree with Xidian University.

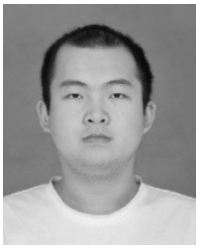

NAN ZHAO is currently pursuing the Ph.D. degree with Xidian University.

MINGMING WANG is currently pursuing the master's degree with Xidian University.

GE GAO is currently pursuing the master's degree with Xidian University.

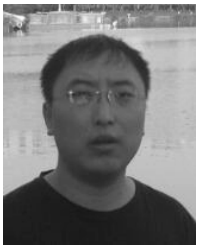

XIAODONG YANG is currently with Xidian University.

ZHIYA ZHANG is currently with Xidian University.

FANGMING HU is currently with Xidian University.

MASOOD UR REHMAN (SM'16) received the B.Sc. degree in electronics and telecommunication engineering from the University of Engineering and Technology, Lahore, Pakistan, in 2004, and the M.Sc. and Ph.D. degrees in electronic engineering from the Queen Mary University of London, London, U.K., in 2006 and 2010, respectively. He was with the Queen Mary University of London as a Post-Doctoral Research Assistant until 2012 before joining the Centre for Wireless Research, University of Bedfordshire, University Square, Luton, U.K., as a Lecturer. He has involved on a number of projects supported by industrial partners and research councils. He has contributed to a patent and authored/co-authored four books, seven book chapters, and over 75 technical articles in leading journals and peer-reviewed conferences. His research interests include compact antenna design, radiowave propagation and channel characterization, satellite navigation system antennas in cluttered environment, electromagnetic wave interaction with human body, body-centric wireless networks and sensors, remote health care technology, mmWave and nanocommunications for body-centric networks, and D2D/H2H communications. He is a fellow of the Higher Education Academy (U.K.), a member of the IET, and a part of the technical program committees and organizing committees of several international conferences, workshops, and special sessions. He is acting as an Associate Editor of the IEEE Access and a lead guest editor of numerous special issues of renowned journals. He also serves as a reviewer for book publishers, IEEE conferences and leading journals.

QAMMER H. ABBASI (SM'16) received the B.Sc. and M.Sc. degrees (Hons.) in electronics and telecommunication engineering from the University of Engineering and Technology (UET), Lahore, Pakistan, and the Ph.D. degree in electronic and electrical engineering from the Queen Mary University of London (QMUL), U.K., in 2012. In 2012, he was a Post-Doctoral Research Assistant with the Antenna and Electromagnetics Group, QMUL, U.K. From 2012 to 2013, he was an International Young Scientist under the National Science Foundation of China, and an Assistant Professor with the University of Engineering and Technology, Lahore. From 2013 to 2017, he was with the Centre for Remote Healthcare Technology and Wireless Research Group, Department of Electrical and Computer Engineering, Texas A &M University (TAMUQ), initially as an Assistant Research Scientist and later was promoted to an Associate Research Scientist and a Visiting Lecturer where he was leading multiple Qatar national research foundation grants (worth $3 million). He is currently a Lecturer (Assistant Professor) with the School of Engineering, University of Glasgow, a Visiting Research Fellow with QMUL, and a Visiting Associate Research Scientist with TAMUQ. He has been mentoring several undergraduate, graduate students, and postdocs. He has contributed to a patent, over 150 leading international technical journal and peer-reviewed conference papers and five books and received several recognitions for his research including the University Research Excellence Award from TAMUQ in two consecutive years, a Reward for Excellence from the University of Glasgow, U.K., and an Exceptional Talent Endorsement by the Royal Academy of Engineering, most downloaded paper in the IEEE Terahertz Transaction, Media coverage by Analog IC tips, Microwaves & RF newsletters, and Vertical news. His research interests include nanocommunication, RF design and radio propagation, biomedical applications of millimeter-wave and terahertz communication, antenna interaction with human body, wearables and implants, nano-scale agri-tech, body centric wireless communication issues, wireless body sensor networks, non-invasive health care solutions, cognitive and cooperative network and multiple-input-multiple-output systems. Since 2012, he has been a member of IET. He has been a member of the technical program committees of several IEEE flagship conferences and a technical reviewer for several IEEE and top-notch journals. He contributed in organizing several IEEE conferences, workshop, and special sessions in addition to European school of antenna course. He is an Associate Editor of the IEEE Access journal, the IEEE Journal of Electromagnetics, RF and Microwaves in Medicine and Biology, and acted as a guest editor for numerous special issues in top notch journals.